

Photocopy and Use Authorization

In presenting this thesis in partial fulfillment of the requirements for an advanced degree at Idaho State University, I agree that the Library shall make it freely available for inspection. I further state that permission for extensive copying of my thesis for scholarly purposes may be granted by the Dean of the Graduate School, Dean of my academic division, or by the University Librarian. It is understood that any copying or publication of this thesis for financial gain shall not be allowed without my written permission.

Signature _____

Date _____

A comparative analysis of intramuscularly and intravenously injected plutonium to the wound
retentions as listed in chapter 4 of *NCRP Report No. 156*

by

Jeremiah Sauber

A thesis

submitted in partial fulfillment

of the requirements for the degree of

Master of Science in the Department of Nuclear Engineering

Idaho State University

Spring 2019

Committee Approval

To the Graduate Faculty:

The members of the committee appointed to examine the thesis of JEREMIAH SAUBER find it satisfactory and recommend that it be accepted.

Name,
Major Advisor

Name,
Committee Member

Name,
Graduate Faculty Representative

Table of Contents

List of Figures	vi
List of Tables	vii
List of Abbreviations	viii
Abstract	ix
Chapter I: Introduction.....	1
Overview.....	1
NCRP 156 Biokinetic Wound Model	3
Supporting Studies of Intramuscularly Injected Plutonium Solutions.....	9
Health Effects: Studies of Pu-238 Uptakes in Workers.....	10
Objectives	12
Hypothesis Testing.....	13
Chapter II: Methods and Materials	14
Collection Protocol	14
Test Subjects	16
Data Analysis	17
Case Selection.....	18
Case Analysis.....	18
Chapter III: Results and Discussion.....	20

Results.....	20
Discussion.....	26
Conclusions.....	28
References.....	29
Appendix A.....	32

List of Figures

Figure 1.1: NCRP 156 Wound Model.	3
Figure 1.2: Human Skin Layers.	6
Figure 1.3: Retention Fractions vs. Days.	7
Figure 3.1: Intramuscular Retention Fraction vs Time.	21
Figure 3.2: Intravenous Retention Fraction vs Time.	22
Figure 3.3: Difference (i.m. - i.v.) vs Time.	23
Figure 3.4: Wound Site Retention vs Time.	24
Figure 3.5: Wound Site Retention Fraction vs Time.	25

List of Tables

Table 2.1: Measured Retentions.	19
Table A1: Necropsy Retention Fractions.	32
Table A2: Percent Differences Between NCRP-156 Weak Retention Equation and Difference (i.m. - i.v.).	34

List of Abbreviations

CIS	Colloid and Intermediate State
IM	Intramuscular
IV	Intravenous
NCRP	National Council of Radiation Protection
PAB	Particles, Aggregates, and Bound state
TPA	Trapped Particles and Aggregates

A comparative analysis of intramuscularly and intravenously injected plutonium to the wound retentions as listed in chapter 4 of *NCRP Report No. 156*

Thesis Abstract – Idaho State University (2019)

This research compared the data sets of intramuscularly injected plutonium and intravenously injected plutonium to the wound retentions as listed in chapter 4 of NCRP Report No. 156. The retention at the injection site within the muscles was hypothesized to be the difference between the lines of best fit for the intramuscular injection data and the intravenous injection data. This difference was compared to the most closely fitting NCRP-156 retention equation, the weak retention equation, and the percent difference were calculated. These data were found to not be a fit for the retention equations.

Key Words: Plutonium, NCRP-156, Wound Model, Nonhuman Primate

CHAPTER 1. INTRODUCTION

1.1 OVERVIEW

Plutonium is an actinide that was the first human-made element to be synthesized in sufficient amounts to be weighed. It was first synthesized by deuteron bombardment of uranium by Seaborg and co-workers in 1940. The alpha-emitting Pu-238 and Pu-239 isotopes are the isotopes of plutonium that are most commonly encountered and widely studied. Pu-239 was first used in fission weapons and one-third of the total energy produced in commercial nuclear power reactors comes from Pu-239 fission. Pu-238 is produced in nuclear fuel and has been used as a heat source in nuclear batteries to produce electricity in unmanned spacecraft. (Toxicological Profiles for Plutonium)

The main sources of plutonium in the environment are releases from research facilities, waste disposal, nuclear weapons testing, accidents, and nuclear weapons production. Atmospherically released plutonium settles through wet and dry deposition to surface water and soil. Soluble plutonium can adsorb to soil and sediment particles or bioaccumulate in the food chain. (Toxicological Profiles for Plutonium)

Humans may be exposed to plutonium if exposed to contaminated air, drinking water, food, or injuries. A pathway that has been demonstrated to be important is that of contaminated wounds.

Examples of such plutonium contaminated wounds include the Savannah River National Laboratory Pu puncture incident.

This paper examines the injury pathway by comparing a data set from nonhuman primates to the NCRP 156 wound model.

1.2 NCRP 156 BIOKINETIC WOUND MODEL

The National Council on Radiation Protection and Measurements (NCRP) report No. 156 biokinetic wound model (Figure 1.1) consists of seven compartments, five for the wound site and two for the radioactive material leaving the wound site. The five wound site compartments are comprised of:

- 1) fragment;
- 2) particles, aggregates, and bound state (PAB);
- 3) trapped particles and aggregates (TPA);
- 4) soluble;
- 5) colloid and intermediate state (CIS).

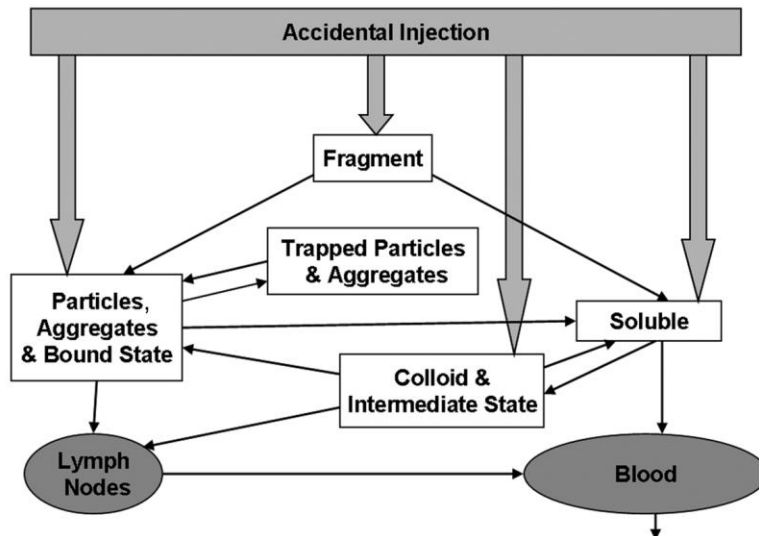


Figure 1.1: NCRP 156 Wound Model.

The NCRP 156 model wound compartments are considered independent of the anatomical location of a wound. NCRP assumes that the nature of most injuries is that they occur in the shallow skin tissue or muscle. The NCRP 156 model does not distinguish between wounds resulting from punctures, abrasions, cuts, or burns; however, the model does note that the level of injury severity will affect the biokinetics of the radionuclide at the wound site. The physical and chemical properties of the radionuclides in the wounds are the basis for each compartmental representation. Radioactive material in the wound site is described as a fragment, particulate, solution form, or in a colloidal state. These transfer compartments are described using first-order kinetics. The default retention categories for the NCRP 156 wound model were established as weak, moderate, strong, and avid (NCRP 2006).

Fragments and particles are considered solids in the NCRP 156 model. Particles are deemed smaller than fragments with an upper limit of 20- μm diameter. Particles may come from corrosion product fragments that the body experiences as contaminated material. The soluble compartment of the wound model represents radionuclides that are introduced in soluble form or originate from the fragment or PABS compartments. Wound data from animal studies suggests that radionuclides in suspension or solution form have a wide range of biokinetic behaviors; thus, three compartments; CIS, PABS, and soluble are used to describe the behavior of contaminants in the wound model. These three solubility-based compartments allow the model more mathematical flexibility for various wounds and differing radionuclides.

Interactions between the CIS and soluble compartments are highly dependent on the radionuclides aqueous chemistry and the potential for a radionuclide complex hydrolyzing within the wound site. The propensity demonstrated by a complex involving a radionuclide for hydrolyzing at the wound determines its persistence in the wound site. As an example, highly charged ions would be expected to bind with fixed tissue constituents. As a contrast, those radionuclides that are associated with a soluble complex in saline have a higher tendency to move to the CIS compartment.

The PABS compartment involves particles, and those compounds in the CIS compartment that have aggregated. Radioactive compounds in the PABS compartment are highly retained at the wound site or they may be transported into the lymph nodes via tissue macrophages (NCRP 2006).

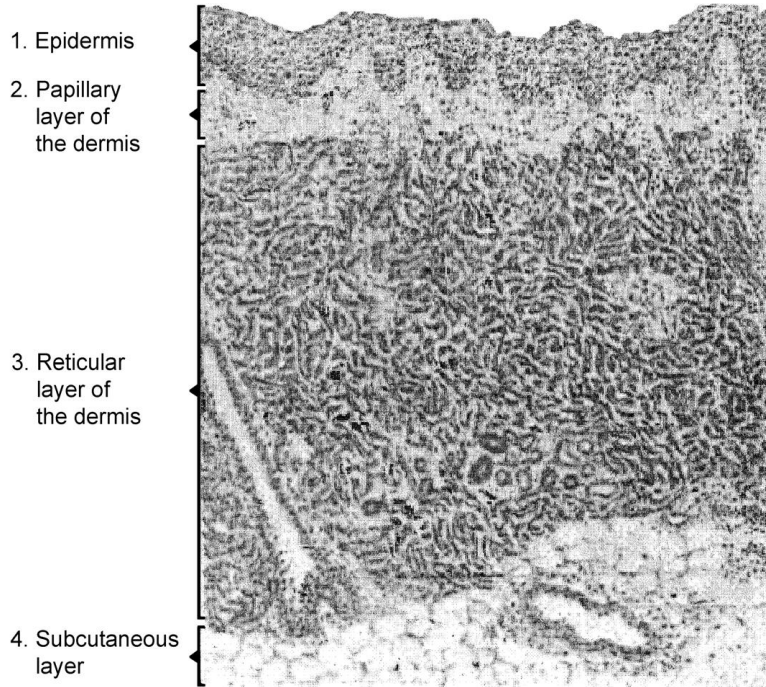


Figure 1.2: Human Skin Layers. (NCRP-156)

The Trapped Particles and Aggregates compartment represents the alternating and dissolution biokinetic nature of particles, or foreign-body reaction, leading to fibrous tissue encapsulation of radioactive materials at the wound site. This foreign-body reaction is dependent on the amount and size of the particles in question at the wound site. The effects of irradiation on the surrounding tissue from the encapsulated radioactive particle have not been fully studied to date. Radioactive material transport from a fragment in the wound is not likely to be a factor due to the slow rate of corrosion of fragments compared to particles. Hence, a separate “trapped fragment” compartment was not included in the wound model (NCRP 2006).

There are four stages of wound healing which generally progress in order: hemostasis, inflammation, proliferation and maturation. Hemostasis is the rapid process of wound closure by clotting by blood vessel constriction, platelet accumulation at the wound, and coagulation. Inflammation is the rapidly on-setting swelling of the wound site which reduces bleeding and infection while providing additional cells that close wounds, fight infection, and repair damage. The proliferative phase is when new tissue comprised of collagen and extracellular matrix rebuilds the wound. And the maturation phase is marked by the remodeling of the collagen and the full closure of the wound.

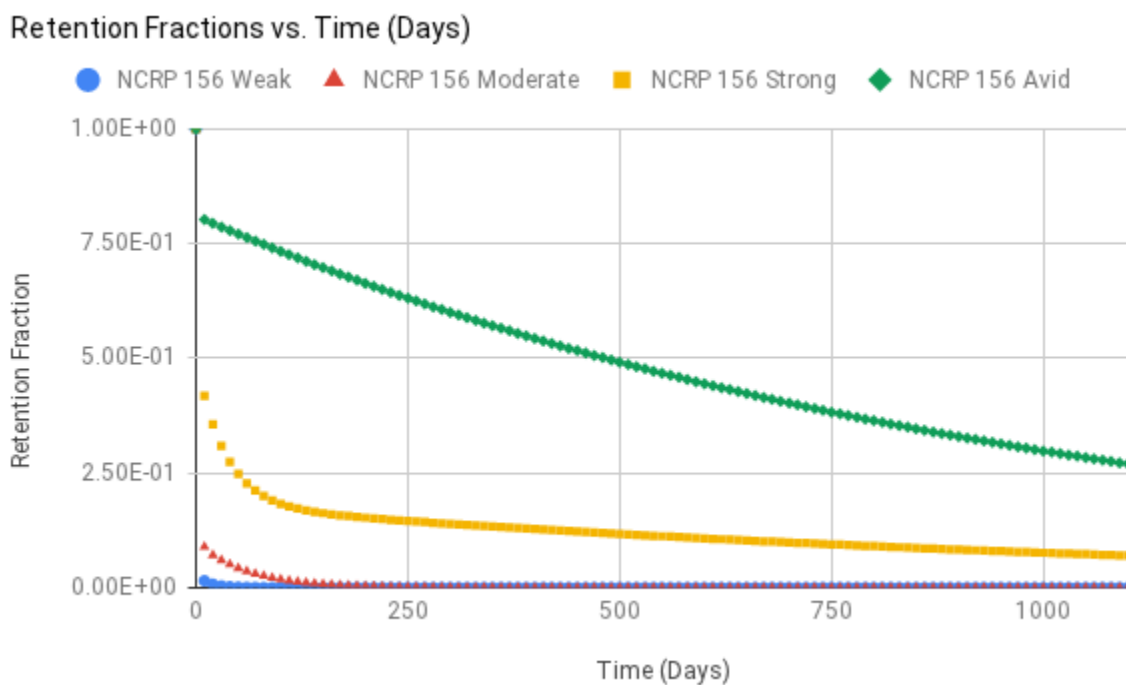


Figure 1.3: Retention Fractions vs. Days. This plot was developed using the ICRP 156 retention equations.

The NCRP 156 retention fractions are plotted in Figure 1.3. The general wound model equations for weak, moderate, strong, and avid retentions are as follows:

$$R(t)_{\text{weak}} = 53e^{-66t} + 44e^{-5.7t} + 3e^{-0.07t} \quad (1)$$

$$R(t)_{\text{moderate}} = 55e^{-47t} + 35e^{-0.43t} + 10e^{-0.017t} \quad (2)$$

$$R(t)_{\text{strong}} = 50e^{-1.1t} + 32e^{-0.029t} + 18e^{-0.00086t} \quad (3)$$

$$R(t)_{\text{avid}} = 19e^{-37t} + 81e^{-0.001t} \quad (4)$$

1.3 SUPPORTING STUDIES OF INTRAMUSCULARLY INJECTED PLUTONIUM SOLUTIONS

NCRP 156 Appendix A.4.1. details several studies of research animals that were intramuscularly injected with radionuclide solutions. Studies of $^{239}\text{Pu}(\text{NO}_3)_4$ intramuscularly injected into animal indicated two retention patterns that depended on the strength of the initial acidic solution. The exact pH of dilute acid and strong acid were not specified in the report. The two patterns were described with the following functions:

$$R(t)_{\text{Dilute Acid}} = 18e^{-4.6t} + 71e^{-0.018t} + 11e^{-0.0025t} \quad (5)$$

$$R(t)_{\text{Strong Acid}} = 8e^{-1.2t} + 21e^{-0.18t} + 72e^{-0.004t} \quad (6)$$

1.4 HEALTH EFFECTS: STUDIES OF PU-238 UPTAKES IN WORKERS

Plutonium may remain in the lungs or move to the bones, liver, or other body organs. As a function of solubility some plutonium may remain in the body for decades and continues to expose the surrounding tissues to radiation. (Toxicological Profiles for Plutonium)

A risk of cancer of the lung, bones, and liver exists and is generally dependent on the quantity and residence time of the plutonium and the resultant dose rate. These cancer types have been observed in workers who had inhalation uptakes at higher levels than the general population. (Toxicological Profiles for Plutonium)

Most of the plutonium body burden is in the skeleton, liver, and lung-associated lymph nodes which results in these tissues receiving the majority of the dose. Toxicity due to radiation has been documented in these tissues in studies of accidents and in animal studies. One unlikely yet possible outcome would be the death. Decreased survival was observed in animal studies, specifically beagle dogs, with plutonium uptakes resulting in initial lung burdens of ≥ 1 kBq/kg body weight. Most early deaths were associated with radiation pneumonitis and decreased life-span was typically associated with tumors. (Suslova, et al, 2012)

Possible correlations between plutonium uptake and cancer mortality and morbidity have been observed in studies of workers at the U.S. plutonium production facilities (Hanford, Los Alamos,

Rocky Flats), and facilities in Russia (Mayak) and the United Kingdom (e.g., Sellafield). The Mayak cohorts had relatively high plutonium uptakes with individual uptakes of up to 470 kBq. These Mayak studies provide evidence for a correlation between increased cancer mortality (lung, liver, bone) and plutonium uptake. Other studies in the U.S. and U.K. resulted in lower correlations between cancer mortality and plutonium uptake. (Toxicological Profiles for Plutonium)

1.5 OBJECTIVES

The primary objective of this research is to compare the data sets of intramuscularly injected plutonium and intravenously injected plutonium to the wound retentions as listed in chapter 4 of NCRP Report No. 156. The retention equations in NCRP 156 are based on data derived from animal studies, mostly rats.

It is evident that plutonium can be measured in the urine and feces and that bioassay data can be used to estimate the total amount of plutonium that has entered the body. Therefore, levels of plutonium in the body can be used to predict the kind of health effects that might develop from that exposure.

Similar studies have been performed on portions of this data set. One study compared the NCRP 156 wound model transfer rate constants to the early blood excretion data from nonhuman primate experiments for Pu-238 and the results indicated a moderate retention in the blood.

1.6 HYPOTHESIS TESTING

NCRP Report No. 156 wound intake retention factor values are expected to accurately predict the simulated Pu-238 wound retention levels from nonhuman primates injected intramuscularly. In order to evaluate the portions of the injections that may be considered to simulate a wound, the differences between the end-of-life retentions from nonhuman primates injected intramuscularly and the end-of-life retentions from nonhuman primates injected intravenously were calculated.

Null hypothesis (H₀): The NCRP Report No. 156 wound retention factors model is correct for the Pu-238 levels.

Alternate hypothesis (H₁): The NCRP Report No. 156 wound retention factors model is not correct for the Pu-238 levels.

The data is consistent with the null hypothesis if the retention equations of NCRP 156 predict the difference in Pu-238 concentration levels within an arbitrarily chosen relative error of 10%; otherwise the data supports the alternative hypothesis.

CHAPTER 2. METHODS AND MATERIALS

2.1 COLLECTION PROTOCOL

At the Division of Research Medicine and Radiation Biophysics at the Lawrence Berkeley Laboratory in Berkeley, California Dr. Patricia W. Durbin and Dr. Nylan Jeung performed uptake and retention experiments investigating Pu-238 translocation in nonhuman primates.

The source material was from 300 mg of $^{238}\text{PuO}_2$ originally separated by the Oak Ridge National Laboratory mass spectrograph on December 20, 1965. At that time it was composed of 99.48% Pu-238, 0.46% Pu-239, 0.036% Pu-240, 0.016% Pu-241, and 0.002% Pu-242. It is known that 2.6×10^8 Bq of activity from the original source was radio-chemically prepared at the University of Utah Radiobiology Laboratory and in 1973 a portion of this stock solution was transferred to the Lawrence Berkeley Laboratory for the Durbin studies.

Between 1973 and 1985, 27 female and male nonhuman primates (*Macaca mulatta*, *Macaca fascicularis*, *Macaca arcuoides*), mainly adults, while under Sernylan and Ketalar anesthesia were given either intravenous or intramuscular injections of Pu-238(IV) in 0.08 M sodium citrate buffer, pH 3.5; of dosages ranging from 11.1 to 72.3 kBq kg⁻¹. Serial blood samples were drawn and all excreta were collected for subsequent radioanalysis. At times ranging from 2 hours to 1,100 days after injection the animals were sacrificed. At necropsy all soft tissues and bones

(many subdivided into compact and cancellous bone components) were removed, weighed, and radioanalyzed.

The excreta data for each nonhuman primate includes the sampling intervals and corresponding Pu-238 fraction for feces and urine during the sampling intervals. Excreta samples were dried at 200°C, weighed, ashed in a furnace at 600°C, and the ash weighed. These samples were alpha counted in a calibrated proportional counter. To improve counting, after the first two weeks, excreta samples were also chemically processed to remove sodium and potassium. Feces and urine were collected separately via screens and pans under cages. Nearly 100% of the injected Pu-238 was accounted for in the excreta, blood samples, and necropsies. After necropsy, tissues and bones were dried at 100°C, weighed, and then ashed in a furnace at 600°C. The ash was again weighed and then alpha counted in a proportional counter.

The gas-flow proportional counter included a preamplifier-discriminator, automatic sample changer, time delay unit, decade scalar, and a printer. The photon detection system was a custom-built scintillation detection system used to count samples containing more than 0.05% of the original injected activity. Calibration information on these detector systems was not listed with the data reports.

2.2 TEST SUBJECTS

Average rhesus macaques are brown or grey in color with a pink face, which is without fur. The tail averages between 20.7 and 22.9 cm. Adult females average about 47 cm in length and 5.3 kg in weight and adult males average about 53 cm in length and about 7.7 kg in weight. Rhesus macaques usually have 50 vertebrae, long arms, dorsal scapulae, and a wide rib cage. They have 32 teeth with bilophodont molars. (Rhesus macaque: *Macaca mulatta*)

Cynomolgus macaques are closely related to rhesus macaques (*Macaca mulatta*). While clearly distinct in body size (cynomolgus macaques are smaller), physiology, and susceptibility to infectious diseases, these two species can form reproductively viable hybrids in the wild.

Rhesus macaques are diurnal animals, and both arboreal and terrestrial. They are quadrupedal and walk digitigrade and plantigrade. They are regular swimmers. They are mostly herbivorous, feeding mainly on fruit, but also eating seeds, roots, buds, bark, and cereals. They are estimated to consume around 99 different plant species from 46 families. They get most of their water from drinking when foraging or from eating fruits. The cynomolgus (*Macaca fascicularis*) is also known to eat crabs, which can be a factor in evaluating intake pathways involving digestion because of differences in biliary excretion. (Rhesus macaque: *Macaca mulatta*)

Due to their relatively easy upkeep in captivity, wide availability, and closeness to humans anatomically and physiologically, they have been used extensively in medical and biological

research on human and animal health-related topics. Because they are relatively small in comparison to other nonhuman primate laboratory species, cynomolgus macaques have been widely used in drug development, drug testing, and toxicology.

2.3 DATA ANALYSIS

These nonhuman primate data are from adult nonhuman primates that were provided radionuclides for uptake via intramuscular injection. The nonhuman primates tested in this study were limited to only those which received intravenous injections or simulated injuries with intramuscular injection and had a remaining life-span of greater than 1 day.

An investigation of the deviation between the closest NCRP 156 Wound Model retention factor equation and the data were conducted using the following two equations:

$$\text{Percent Deviation} = [(\text{Model} - \text{Data}) / (\text{Data})] \times 100\% \quad (7)$$

$$\text{Percent Deviation} = [(\text{Model} - \text{Data}) / (\text{Model})] \times 100\% \quad (8)$$

2.4 CASE SELECTION

The cases selected for this study were nonhuman primates what had been injected with a plutonium solution and from which data was taken for more than one day. Data was actually taken over a span of time of minutes to years but this thesis considers retention over time periods of at least one day.

2.5 CASE ANALYSIS

The cases were analyzed by summing the retentions measured after necropsy, as summarized in Table 2.1 and presented in detail in Appendix A.

Animal#	Injection Mode	Time (days)	Total Retention
S114F	i.m.	7	9.752×10^{-1}
C145M	i.m.	7	9.839×10^{-1}
C131F	i.m.	56	5.438×10^{-1}
R186M	i.m.	103	4.996×10^{-1}
C106M	i.m.	106	6.608×10^{-1}
C166M	i.m.	106	6.610×10^{-1}
C80F	i.m.	1100	1.114×10^{-1}
C89M	i.v.	7	9.686×10^{-1}
R121M	i.v.	7	9.721×10^{-1}
C109F	i.v.	7	9.452×10^{-1}
R119F	i.v.	7	9.717×10^{-1}
R101F	i.v.	8	9.674×10^{-1}
R120M	i.v.	8	9.641×10^{-1}
R122F	i.v.	8	9.677×10^{-1}
R192M	i.v.	8	9.552×10^{-1}
R100F	i.v.	67	6.987×10^{-1}
C79F	i.v.	106	4.877×10^{-1}
C111F	i.v.	173	6.676×10^{-1}
C107M	i.v.	173	6.602×10^{-1}
R99F	i.v.	370	2.670×10^{-1}
C105M	i.v.	552	5.815×10^{-1}
S116F	i.v.	559	2.781×10^{-1}
C94F	i.v.	587	1.114×10^{-1}
R102F	i.v.	1099	2.032×10^{-1}

Table 2.1: Measured Retentions.

CHAPTER 3. RESULTS AND DISCUSSION

3.1 RESULTS

These data did not describe the muscle groups into which the plutonium was intramuscularly injected. To estimate the portion of plutonium that was retained in the intramuscular injection site these data were separated into two groups, intramuscular and intravenous injection. For each of the intramuscularly injected nonhuman primates, the total activity at the time of sacrifice was calculated. Then all of the activities at sacrifice were plotted for the intramuscularly injected nonhuman primates and a trendline was calculated (see Figure 3.1). The same procedure was completed for the intravenously injected nonhuman primates (see Figure 3.2). The difference between the two trendlines was calculated and a trendline of the difference was plotted (see Figure 3.3).

Intramuscular Retention Fraction vs Time (days)

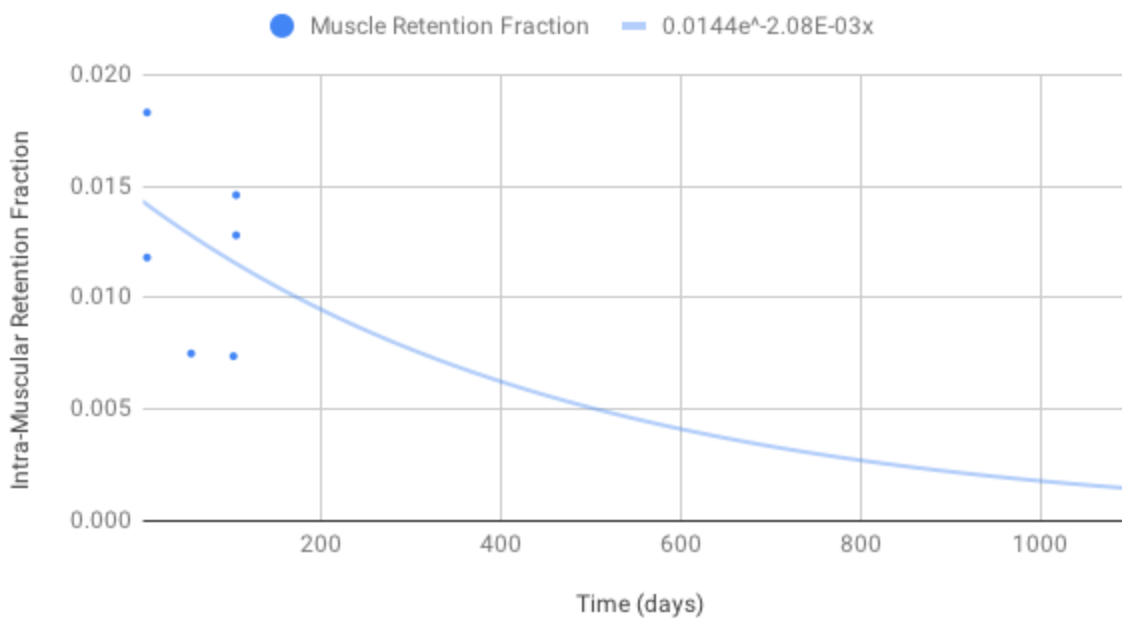


Figure 3.1: Intramuscular Retention Fraction vs Time.

Plotted in Figure 3.1 are the total retentions from nonhuman primates intramuscularly injected with Pu-238. It may be observed that the general trend is as would be expected, that the longer the time from injection the less the retention at the time of necropsy. A trend line was generated for comparison with intravenous injection data.

Intravenous Retention Fraction vs Time (days)

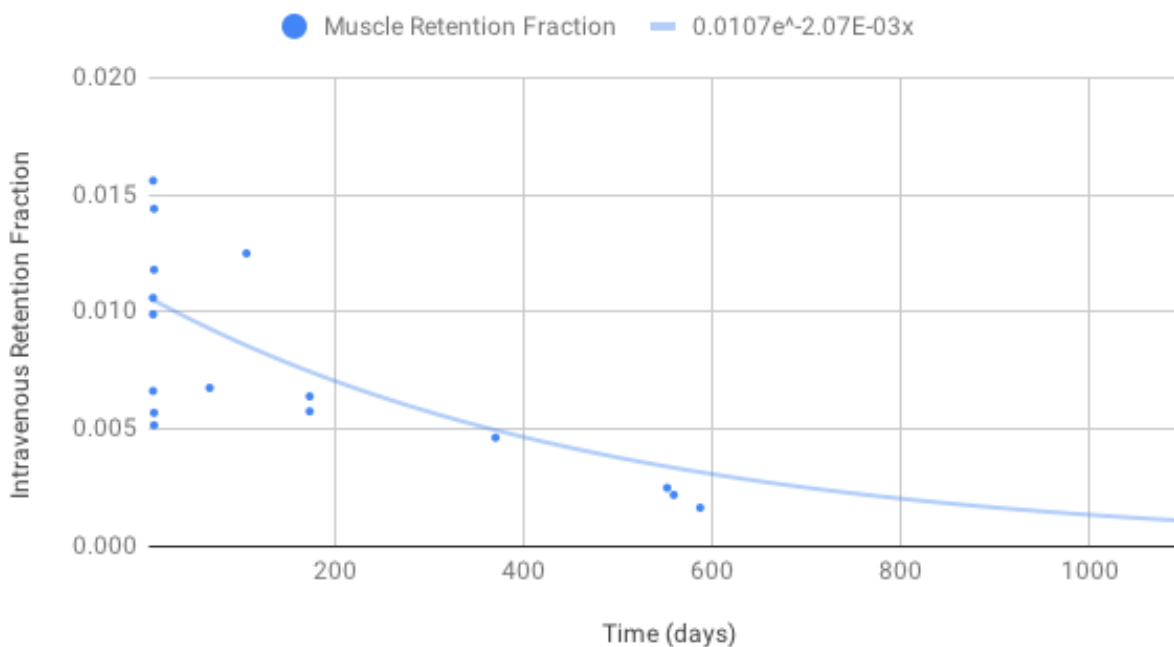


Figure 3.2: Intravenous Retention Fraction vs Time.

Plotted in Figure 3.2 are the total retentions from nonhuman primates intravenously injected with Pu-238. It may be observed that the general trend is as would be expected, that the longer the time from injection the less the retention at the time of necropsy. A trend line was generated for comparison with intramuscular injection data.

Difference (i.m. - i.v.) vs Time (days)

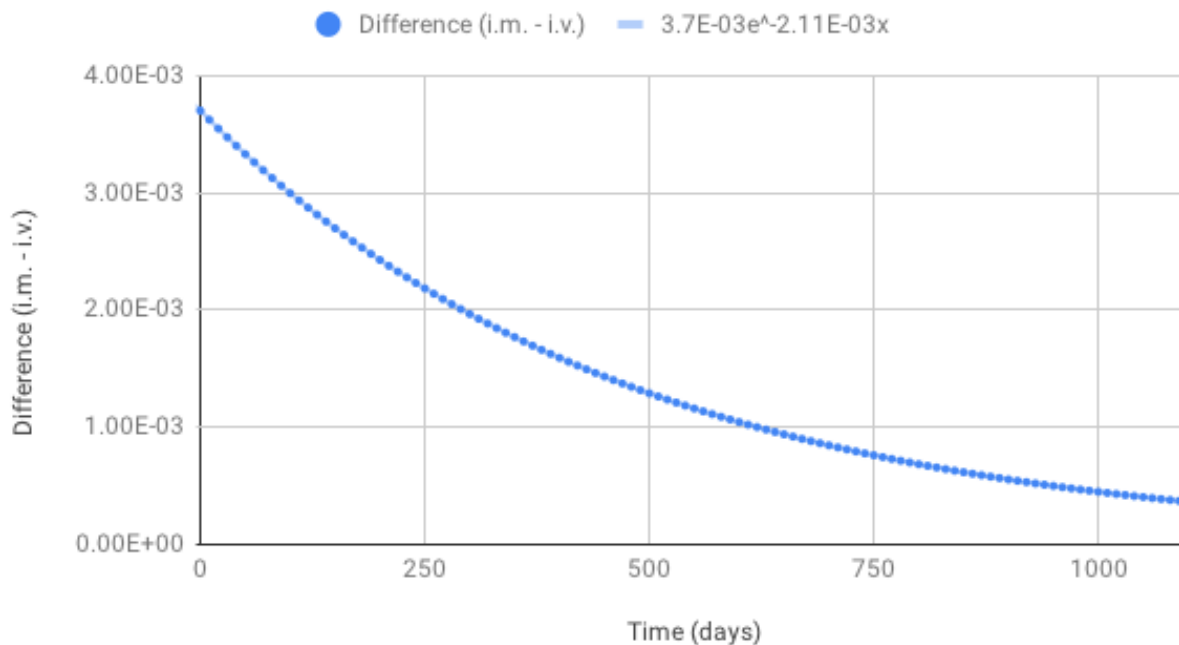


Figure 3.3: Difference (i.m. - i.v.) vs Time.

It may be observed from the plot of the differences between intramuscularly and intravenously injected nonhuman primates that there was some additional retention with intramuscular injection and that this additional retention diminished over time. That there is a difference seems to conform to an expectation that these injection sites would not behave the same. That this difference reduces over time seems to conform to an expectation that this difference would diminish over time as a result of material leaving the injection site and entering the bloodstream. And that the difference is so small seems to conform to an expectation that the method of

injection into the muscles may have flooded the muscle area and not been initially well retained at the injection site.

Wound Site Retention vs Time

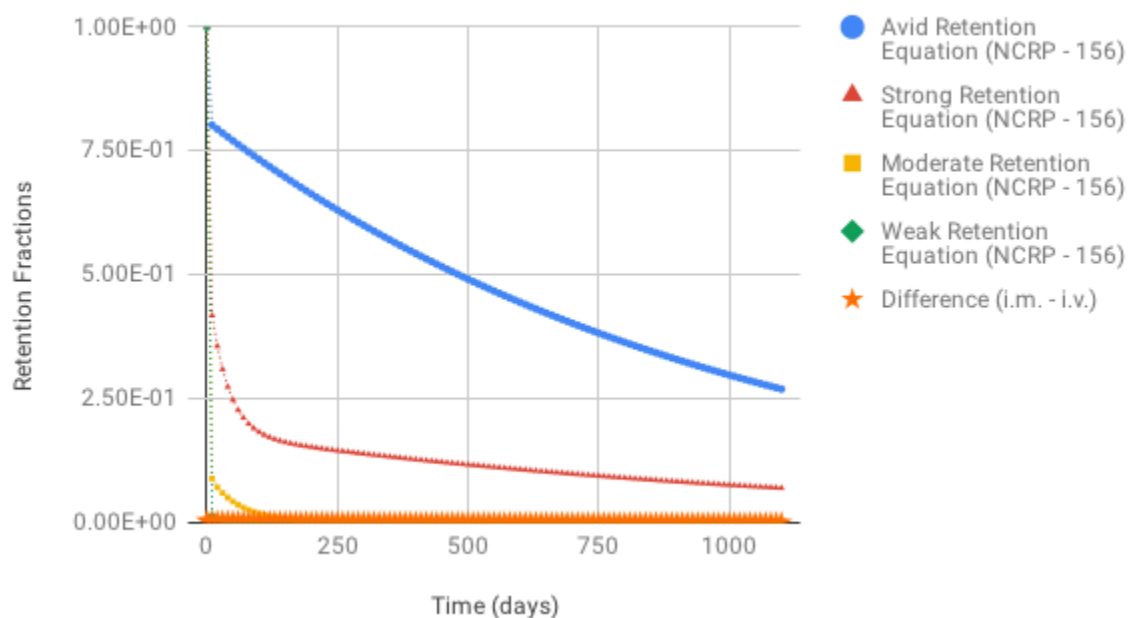


Figure 3.4: Wound Site Retention vs Time.

A comparison of the potential wound site retention to the NCRP-156 wound site retention equations was made (see Figure 3.4). The difference between intramuscular injections and intravenous injections, Difference (i.m. - i.v.), was observed to be similar to the weak retention equation, Weak Retention Equation (NCRP-156).

Wound Site Retention Fraction vs Time

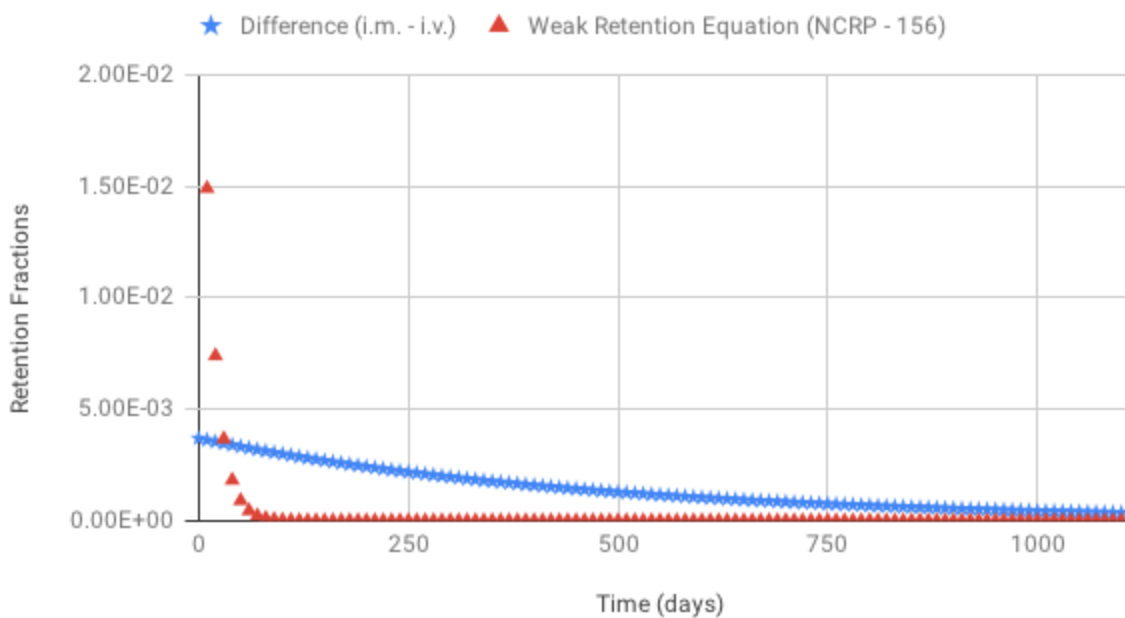


Figure 3.5: Wound Site Retention Fraction vs Time.

A comparison of the potential wound site retention to the NCRP-156 wound site weak retention equation was made (see Figure 3.5). It may be observed that the wound site retention may be close to the weak retention equation. By visual inspection it is clear that the difference between intramuscular and intravenous injections is not a match for any of the NCRP-156 wound site retention equations and fails the percent difference test for a comparison between these data and the weak retention equation, with the calculated percent differences between intramuscular and intravenous injections varying from each other by more than the hypothesis test criteria (see Table A2).

3.2 DISCUSSION

Our ability to model fecal excretion from nonhuman primates using compartmental models designed for is likely to be a limiting factor to the accuracy of this approach. Most nonhuman primates in this genus are strictly vegetarian, with one species known to eat some crabs. One of the consequences of this difference in diet is that the bile excretion is much different from that of humans and they have evolved longer intestines. The bile duct excretes bile salts in the proximal end of the small intestine, and in humans these salts help to emulsify fats. These difference result in difficulties predicting fecal excretion with nonhuman primate data when comparing or using human clearance rates in the ICRP 156 Wound Model.

In the case of these data, the average lymph node retention for intramuscular injection was 3.36×10^{-5} and for intravenous injection was 1.54×10^{-4} , which runs counter to the expectations of wound-like behavior. If the administered plutonium was found to not be retained at the site of injection like a wound, then it might be retained like a drug injection. Intramuscular injection is known to deliver a drug into the muscle tissue where the drug is absorbed into the blood vessels, often quickly, and this method is commonly used to deliver vaccinations. Intravenous injection is known to be the fastest route of entry into the bloodstream and is the most common method of drug administration. Comparative studies have been done to compare intravenous and

intramuscular injection methods and the results were that it depends on the pharmacokinetics of the drug being administered (Zhu, et al, Patient Preference Adherence).

3.3 CONCLUSIONS

These data support the alternative hypothesis, that the NCRP Report No. 156 wound retention factors model is not correct for the Pu-238 levels calculated as the difference between intramuscular and intravenous injections. These data from the intramuscular injection of nonhuman primates with Pu-238 are not a fit for the NCRP-156 Wound Model. The differences between intramuscular and intravenous activities represent the activities involved in the simulated wounds which are not immediately available to the transfer compartments of the blood and body. But the NCRP-156 wound model does not adequately describe the small difference between the behavior of intramuscular and intravenous injections. This difference was speculated to reflect minor tissue damage in the muscle, i.e. a wound, using intramuscular injection information as a surrogate for wound data has not been supported by this analysis considering plutonium citrate injections. If the NCRP-156 wound model equations were used for this data set to predict committed effective dose equivalent, the result would be a significant overprediction of dose.

REFERENCES

1. National Council on Radiation Protection and Measurements. Development of a Biokinetic Model for Radionuclide-Contaminated Wounds and Procedures for their assessment, dosimetry, and Treatment. Bethesda, MD: NCRP Report No. 156; 2006.
2. Durbin, PW, Jeung, N. Collected Original Data on Distribution of Plutonium-238 in Soft Tissues and Bones of Monkeys. Berkeley, CA: Lawrence Berkeley Laboratory; Division of Research Medicine and Radiation Biophysics; March 1990.
3. Poudel, D, Guilmette, RA, Klumpp, JA, Bertelli, L, Waters, TL. Application of NCRP 156 Wound Models for the Analysis of Bioassay Data from Plutonium Wound Cases. Health Physics: Volume 113; Issue 3, pp 209-219; September 2017.
4. Public Health Service Agency for Toxic Substances and Disease Registry. Toxicological Profiles for Plutonium. Washington, DC: U.S. Department of Health and Human Services; November 2010.
5. Suslova, KG, Khokhryakov, VF, Sokolova, AB, Miller, SC. Pu-238: A Review of the Biokinetics, Dosimetry, and Implications for Human Exposures. Health Physics: Volume 102; Issue 3, pp 251-262; March 2012.
6. Eisenbud, M, Gesell, T. Environmental Radioactivity from Natural, Industrial, and Military Sources, Fourth Edition. San Diego, CA: Academic Press; 1997.
7. Martin, JE. Physics for Radiation Protection. Weinheim, Germany: Wiley; 2013.
8. Cember, H. Introduction to Health Physics, Third Edition. New York: McGraw-Hill; 1996.

9. Turner, JE. Atoms, Radiation, and Radiation Protection, Second Edition. New York: Wiley-Interscience; 1995.
10. Skrable, K, French, C, Chabot, G, Tries, M. Fecal Monitoring for Plutonium and Other Long-Lived Actinides Including Methods for Separating the Respirable from the Non-respirable Portion of an Inhalation Intake; From Practical Applications of Internal Dosimetry, Bolch, Wesley E. Editor. Madison, WI: Health Physics Society 2002 Summer School; Medical Physics Publishing; 2002.
11. Poudel, D, Guilmette, RA, Konzen, K, Krage, ES, Brey, RR. Application of NCRP 156 Wound Model and ICRP 67 Systemic Plutonium Model for Analysis of Urine Data from Simulated Wounds in Nonhuman Primates. Health Physics: Volume 111; Issue 1, pp 58-63; July 2016.
12. Konzen, K, Brey, R, Guilmette, R. Early Blood Plutonium Retention in Nonhuman Primates Compared to the NCRP Wound Biokinetic Model. Health Physics: Volume 108; Issue 3, pp 383-387; March 2015.
13. Gebo, DL. Primate Comparative Anatomy. Baltimore, MD: Johns Hopkins University Press; 2014
14. Fleagle, JG. Primate Adaptation and Evolution. San Diego, CA: Academic Press; 2014.
15. Lang, KC. Rhesus macaque: *Macaca mulatta*. Madison, WI: National Primate Research Center; University of Wisconsin - Madison; 2005.
16. Weller, RE, Fisher, DR. Carcinogenesis From Inhaled $^{239}\text{PuO}_2$ in Beagles: Evidence for Radiation Homeostasis at Low Doses. Health Physics 99(3):357–362; 2010.

17. Konzen, K, Brey, R, Guilmette, R. Early Blood Plutonium Retention in Nonhuman Primates Compared to the NCRP 156 Wound Biokinetic Model. *Health Physics* 108(3):383–387; 2015.
18. Poudel, D, Guilmette, RA, Gesell, TF, Harris, JT, Brey, RR. Biokinetics of Plutonium in Nonhuman Primates. *Health Physics: Volume 111 - Issue 4 - p 348–356; October 2016.*
19. Jin, J, Zhu, L, Chen, M, Xu, H, Wang, H, Feng, X, Zhu, X, Zhou, X. The optimal choice of medication administration route regarding intravenous, intramuscular, and subcutaneous injection. *Patient Prefer Adherence: 2015; 9: 923–942.*
20. Nguyen, DT, Orgill, DP, Murphy, GF. The Pathophysiologic Basis for Wound Healing and Cutaneous Regeneration: *Biomaterials for Treating Skin Loss: Chapter 4.*

APPENDIX A: DATA TABLES

Animal#	S114F	C145M	C131F	R186M	C106M	C166M	C80F
Mode	i.m.						
Time (days)	7	7	56	103	106	106	1100
Liver	6.630x10 ⁻¹	7.550x10 ⁻¹	3.350x10 ⁻¹	2.020x10 ⁻¹	4.200x10 ⁻¹	4.240x10 ⁻¹	4.700x10 ⁻³
Kidneys	8.070x10 ⁻³	7.800x10 ⁻³	9.400x10 ⁻⁴	1.020x10 ⁻³	1.800x10 ⁻³	1.650x10 ⁻³	3.600x10 ⁻⁴
Spleen	2.660x10 ⁻³	5.400x10 ⁻³	2.700x10 ⁻³	1.300x10 ⁻³	7.400x10 ⁻⁴	7.100x10 ⁻⁴	9.200x10 ⁻⁶
Muscle	1.830x10 ⁻²	1.180x10 ⁻²	7.500x10 ⁻³	7.380x10 ⁻³	1.460x10 ⁻²	1.280x10 ⁻²	1.490x10 ⁻³
Pelt	8.300x10 ⁻³	8.200x10 ⁻³	3.100x10 ⁻³	3.710x10 ⁻³	5.980x10 ⁻³	4.580x10 ⁻³	6.140x10 ⁻⁴
Gonads	3.000x10 ⁻⁵	1.270x10 ⁻³	1.000x10 ⁻⁵	6.880x10 ⁻⁴	9.300x10 ⁻⁴	9.000x10 ⁻⁴	1.380x10 ⁻⁵
Soft Tissue Balance	1.440x10 ⁻²	1.460x10 ⁻²	6.550x10 ⁻³	6.630x10 ⁻³	6.140x10 ⁻³	6.550x10 ⁻³	2.670x10 ⁻³
Bones	2.590x10 ⁻¹	1.730x10 ⁻¹	1.850x10 ⁻¹	2.720x10 ⁻¹	2.060x10 ⁻¹	2.050x10 ⁻¹	9.890x10 ⁻²
Teeth	9.500x10 ⁻⁴	1.290x10 ⁻³	1.800x10 ⁻³	1.200x10 ⁻³	1.460x10 ⁻³	1.420x10 ⁻³	1.600x10 ⁻³
Tail	4.600x10 ⁻⁴	5.500x10 ⁻³	1.200x10 ⁻³	3.630x10 ⁻³	3.180x10 ⁻³	3.380x10 ⁻³	1.070x10 ⁻³
Total Retention	9.752x10 ⁻¹	9.839x10 ⁻¹	5.438x10 ⁻¹	4.996x10 ⁻¹	6.608x10 ⁻¹	6.610x10 ⁻¹	1.114x10 ⁻¹

Animal#	C89M	R121M	C109F	R119F	R101F	R120M	R122F
Mode	i.v.						
Time (days)	7	7	7	7	8	8	8
Liver	6.240x10 ⁻¹	5.340x10 ⁻¹	6.050x10 ⁻¹	5.490x10 ⁻¹	5.120x10 ⁻¹	6.900x10 ⁻¹	6.080x10 ⁻¹
Kidneys	6.800x10 ⁻³	2.700x10 ⁻³	5.300x10 ⁻³	3.820x10 ⁻³	5.340x10 ⁻³	4.620x10 ⁻³	2.700x10 ⁻³
Spleen	1.500x10 ⁻³	1.720x10 ⁻³	3.600x10 ⁻³	1.600x10 ⁻³	1.150x10 ⁻³	0.000x10 ⁺⁰	1.000x10 ⁻³
Muscle	9.900x10 ⁻³	6.630x10 ⁻³	1.560x10 ⁻²	1.060x10 ⁻²	1.180x10 ⁻²	5.170x10 ⁻³	5.700x10 ⁻³
Pelt	5.500x10 ⁻³	4.430x10 ⁻³	9.100x10 ⁻³	4.400x10 ⁻³	8.330x10 ⁻³	5.770x10 ⁻³	5.200x10 ⁻³
Gonads	3.560x10 ⁻⁴	4.000x10 ⁻⁴	6.000x10 ⁻⁵	4.800x10 ⁻⁵	8.400x10 ⁻⁵	0.000x10 ⁺⁰	3.100x10 ⁻⁵
Soft Tissue Balance	8.100x10 ⁻³	1.250x10 ⁻²	1.750x10 ⁻²	7.760x10 ⁻³	1.510x10 ⁻²	4.200x10 ⁻³	6.780x10 ⁻³
Bones	3.090x10 ⁻¹	4.000x10 ⁻¹	2.800x10 ⁻¹	3.870x10 ⁻¹	4.080x10 ⁻¹	2.480x10 ⁻¹	3.310x10 ⁻¹
Teeth	1.500x10 ⁻³	2.500x10 ⁻³	1.880x10 ⁻³	2.180x10 ⁻³	1.200x10 ⁻³	3.290x10 ⁻³	1.720x10 ⁻³
Tail	1.900x10 ⁻³	7.200x10 ⁻³	7.200x10 ⁻³	5.340x10 ⁻³	4.420x10 ⁻³	3.030x10 ⁻³	5.600x10 ⁻³
Total Retention	9.686x10 ⁻¹	9.721x10 ⁻¹	9.452x10 ⁻¹	9.717x10 ⁻¹	9.674x10 ⁻¹	9.641x10 ⁻¹	9.677x10 ⁻¹

Animal#	R192M	R100F	C79F	C111F	C107M	R99F	C105M
Mode	i.v.						
Time (days)	8	67	106	173	173	370	552
Liver	7.600×10^{-1}	3.650×10^{-1}	2.510×10^{-1}	4.000×10^{-1}	4.300×10^{-1}	4.150×10^{-2}	4.250×10^{-1}
Kidneys	2.440×10^{-3}	1.510×10^{-3}	1.700×10^{-3}	2.000×10^{-3}	$0.000 \times 10^{+0}$	4.300×10^{-4}	1.500×10^{-3}
Spleen	1.330×10^{-3}	1.270×10^{-3}	2.600×10^{-3}	4.160×10^{-3}	2.660×10^{-3}	4.400×10^{-4}	1.000×10^{-3}
Muscle	1.440×10^{-2}	6.760×10^{-3}	1.250×10^{-2}	6.400×10^{-3}	5.760×10^{-3}	4.640×10^{-3}	2.500×10^{-3}
Pelt	6.800×10^{-3}	2.110×10^{-3}	7.200×10^{-3}	2.870×10^{-3}	4.920×10^{-3}	3.260×10^{-3}	2.600×10^{-3}
Gonads	5.760×10^{-4}	3.090×10^{-5}	1.000×10^{-4}	2.050×10^{-5}	2.400×10^{-4}	4.300×10^{-6}	1.890×10^{-4}
Soft Tissue Balance	1.390×10^{-2}	5.580×10^{-3}	9.270×10^{-3}	4.800×10^{-3}	4.200×10^{-3}	2.710×10^{-3}	3.390×10^{-3}
Bones	1.540×10^{-1}	3.120×10^{-1}	1.970×10^{-1}	2.420×10^{-1}	2.070×10^{-1}	2.110×10^{-1}	1.410×10^{-1}
Teeth	5.700×10^{-4}	1.760×10^{-3}	3.200×10^{-3}	1.570×10^{-3}	1.400×10^{-3}	1.700×10^{-3}	1.460×10^{-3}
Tail	1.200×10^{-3}	2.700×10^{-3}	3.100×10^{-3}	3.760×10^{-3}	3.990×10^{-3}	1.270×10^{-3}	2.820×10^{-3}
Total Retention	9.552×10^{-1}	6.987×10^{-1}	4.877×10^{-1}	6.676×10^{-1}	6.602×10^{-1}	2.670×10^{-1}	5.815×10^{-1}

Animal#	S116F	C94F	R102F
Mode	i.v.	i.v.	i.v.
Time (days)	559	587	1099
Liver	1.370×10^{-1}	2.820×10^{-2}	7.700×10^{-3}
Kidneys	1.800×10^{-4}	4.300×10^{-4}	5.400×10^{-5}
Spleen	3.520×10^{-3}	3.900×10^{-4}	1.260×10^{-4}
Muscle	2.200×10^{-3}	1.650×10^{-3}	2.240×10^{-3}
Pelt	1.500×10^{-3}	1.440×10^{-3}	5.500×10^{-4}
Gonads	1.730×10^{-5}	1.100×10^{-5}	6.600×10^{-6}
Soft Tissue Balance	3.800×10^{-3}	3.100×10^{-3}	1.680×10^{-3}
Bones	1.270×10^{-1}	7.350×10^{-2}	1.860×10^{-1}
Teeth	2.550×10^{-3}	1.500×10^{-3}	2.430×10^{-3}
Tail	3.400×10^{-4}	1.170×10^{-3}	2.450×10^{-3}
Total Retention	2.781×10^{-1}	1.114×10^{-1}	2.032×10^{-1}

Table A1: Necropsy Retention Fractions.

Time (days)	Difference (i.m. - i.v.)	Weak Retention Equation (NCRP - 156)	Percent Difference (Model- Data)/(Data)	Percent Difference (Model- Data)/(Model)
0	3.70x10 ⁻⁰³	1.00x10 ⁺⁰⁰	26927.03%	99.63%
10	3.62x10 ⁻⁰³	1.49x10 ⁻⁰²	311.22%	99.52%
20	3.55x10 ⁻⁰³	7.40x10 ⁻⁰³	108.56%	99.32%
30	3.47x10 ⁻⁰³	3.67x10 ⁻⁰³	5.77%	93.64%
40	3.40x10 ⁻⁰³	1.82x10 ⁻⁰³	-46.35%	100.39%
50	3.33x10 ⁻⁰³	9.06x10 ⁻⁰⁴	-72.79%	100.12%
60	3.26x10 ⁻⁰³	4.50x10 ⁻⁰⁴	-86.20%	100.05%
70	3.19x10 ⁻⁰³	2.23x10 ⁻⁰⁴	-93.00%	100.02%
80	3.13x10 ⁻⁰³	1.11x10 ⁻⁰⁴	-96.45%	100.01%
90	3.06x10 ⁻⁰³	5.51x10 ⁻⁰⁵	-98.20%	100.01%
100	3.00x10 ⁻⁰³	2.74x10 ⁻⁰⁵	-99.09%	100.00%
110	2.93x10 ⁻⁰³	1.36x10 ⁻⁰⁵	-99.54%	100.00%
120	2.87x10 ⁻⁰³	6.75x10 ⁻⁰⁶	-99.77%	100.00%
130	2.81x10 ⁻⁰³	3.35x10 ⁻⁰⁶	-99.88%	100.00%
140	2.75x10 ⁻⁰³	1.66x10 ⁻⁰⁶	-99.94%	100.00%
150	2.70x10 ⁻⁰³	8.26x10 ⁻⁰⁷	-99.97%	100.00%
160	2.64x10 ⁻⁰³	4.10x10 ⁻⁰⁷	-99.98%	100.00%
170	2.59x10 ⁻⁰³	2.04x10 ⁻⁰⁷	-99.99%	100.00%
180	2.53x10 ⁻⁰³	1.01x10 ⁻⁰⁷	-100.00%	100.00%
190	2.48x10 ⁻⁰³	5.02x10 ⁻⁰⁸	-100.00%	100.00%
200	2.43x10 ⁻⁰³	2.49x10 ⁻⁰⁸	-100.00%	100.00%
210	2.38x10 ⁻⁰³	1.24x10 ⁻⁰⁸	-100.00%	100.00%
220	2.33x10 ⁻⁰³	6.15x10 ⁻⁰⁹	-100.00%	100.00%
230	2.28x10 ⁻⁰³	3.05x10 ⁻⁰⁹	-100.00%	100.00%
240	2.23x10 ⁻⁰³	1.52x10 ⁻⁰⁹	-100.00%	100.00%
250	2.18x10 ⁻⁰³	7.53x10 ⁻¹⁰	-100.00%	100.00%
260	2.14x10 ⁻⁰³	3.74x10 ⁻¹⁰	-100.00%	100.00%
270	2.09x10 ⁻⁰³	1.86x10 ⁻¹⁰	-100.00%	100.00%
280	2.05x10 ⁻⁰³	9.22x10 ⁻¹¹	-100.00%	100.00%
290	2.01x10 ⁻⁰³	4.58x10 ⁻¹¹	-100.00%	100.00%
300	1.97x10 ⁻⁰³	2.27x10 ⁻¹¹	-100.00%	100.00%
310	1.92x10 ⁻⁰³	1.13x10 ⁻¹¹	-100.00%	100.00%
320	1.88x10 ⁻⁰³	5.61x10 ⁻¹²	-100.00%	100.00%
330	1.84x10 ⁻⁰³	2.79x10 ⁻¹²	-100.00%	100.00%
340	1.81x10 ⁻⁰³	1.38x10 ⁻¹²	-100.00%	100.00%
350	1.77x10 ⁻⁰³	6.87x10 ⁻¹³	-100.00%	100.00%
360	1.73x10 ⁻⁰³	3.41x10 ⁻¹³	-100.00%	100.00%
370	1.70x10 ⁻⁰³	1.69x10 ⁻¹³	-100.00%	100.00%
380	1.66x10 ⁻⁰³	8.41x10 ⁻¹⁴	-100.00%	100.00%

Time (days)	Difference (i.m. - i.v.)	Weak Retention Equation (NCRP - 156)	Percent Difference (Model- Data)/(Data)	Percent Difference (Model- Data)/(Model)
390	1.63x10 ⁻⁰³	4.18x10 ⁻¹⁴	-100.00%	100.00%
400	1.59x10 ⁻⁰³	2.07x10 ⁻¹⁴	-100.00%	100.00%
410	1.56x10 ⁻⁰³	1.03x10 ⁻¹⁴	-100.00%	100.00%
420	1.53x10 ⁻⁰³	5.12x10 ⁻¹⁵	-100.00%	100.00%
430	1.49x10 ⁻⁰³	2.54x10 ⁻¹⁵	-100.00%	100.00%
440	1.46x10 ⁻⁰³	1.26x10 ⁻¹⁵	-100.00%	100.00%
450	1.43x10 ⁻⁰³	6.26x10 ⁻¹⁶	-100.00%	100.00%
460	1.40x10 ⁻⁰³	3.11x10 ⁻¹⁶	-100.00%	100.00%
470	1.37x10 ⁻⁰³	1.54x10 ⁻¹⁶	-100.00%	100.00%
480	1.34x10 ⁻⁰³	7.67x10 ⁻¹⁷	-100.00%	100.00%
490	1.32x10 ⁻⁰³	3.81x10 ⁻¹⁷	-100.00%	100.00%
500	1.29x10 ⁻⁰³	1.89x10 ⁻¹⁷	-100.00%	100.00%
510	1.26x10 ⁻⁰³	9.39x10 ⁻¹⁸	-100.00%	100.00%
520	1.24x10 ⁻⁰³	4.66x10 ⁻¹⁸	-100.00%	100.00%
530	1.21x10 ⁻⁰³	2.32x10 ⁻¹⁸	-100.00%	100.00%
540	1.18x10 ⁻⁰³	1.15x10 ⁻¹⁸	-100.00%	100.00%
550	1.16x10 ⁻⁰³	5.71x10 ⁻¹⁹	-100.00%	100.00%
560	1.14x10 ⁻⁰³	2.84x10 ⁻¹⁹	-100.00%	100.00%
570	1.11x10 ⁻⁰³	1.41x10 ⁻¹⁹	-100.00%	100.00%
580	1.09x10 ⁻⁰³	6.99x10 ⁻²⁰	-100.00%	100.00%
590	1.07x10 ⁻⁰³	3.47x10 ⁻²⁰	-100.00%	100.00%
600	1.04x10 ⁻⁰³	1.72x10 ⁻²⁰	-100.00%	100.00%
610	1.02x10 ⁻⁰³	8.57x10 ⁻²¹	-100.00%	100.00%
620	1.00x10 ⁻⁰³	4.25x10 ⁻²¹	-100.00%	100.00%
630	9.80x10 ⁻⁰⁴	2.11x10 ⁻²¹	-100.00%	100.00%
640	9.59x10 ⁻⁰⁴	1.05x10 ⁻²¹	-100.00%	100.00%
650	9.39x10 ⁻⁰⁴	5.21x10 ⁻²²	-100.00%	100.00%
660	9.20x10 ⁻⁰⁴	2.59x10 ⁻²²	-100.00%	100.00%
670	9.00x10 ⁻⁰⁴	1.28x10 ⁻²²	-100.00%	100.00%
680	8.82x10 ⁻⁰⁴	6.38x10 ⁻²³	-100.00%	100.00%
690	8.63x10 ⁻⁰⁴	3.17x10 ⁻²³	-100.00%	100.00%
700	8.45x10 ⁻⁰⁴	1.57x10 ⁻²³	-100.00%	100.00%
710	8.28x10 ⁻⁰⁴	7.81x10 ⁻²⁴	-100.00%	100.00%
720	8.10x10 ⁻⁰⁴	3.88x10 ⁻²⁴	-100.00%	100.00%
730	7.93x10 ⁻⁰⁴	1.93x10 ⁻²⁴	-100.00%	100.00%
740	7.77x10 ⁻⁰⁴	9.56x10 ⁻²⁵	-100.00%	100.00%
750	7.61x10 ⁻⁰⁴	4.75x10 ⁻²⁵	-100.00%	100.00%
760	7.45x10 ⁻⁰⁴	2.36x10 ⁻²⁵	-100.00%	100.00%

Time (days)	Difference (i.m. - i.v.)	Weak Retention Equation (NCRP - 156)	Percent Difference (Model- Data)/(Data)	Percent Difference (Model- Data)/(Model)
770	7.29x10 ⁻⁰⁴	1.17x10 ⁻²⁵	-100.00%	100.00%
780	7.14x10 ⁻⁰⁴	5.82x10 ⁻²⁶	-100.00%	100.00%
790	6.99x10 ⁻⁰⁴	2.89x10 ⁻²⁶	-100.00%	100.00%
800	6.84x10 ⁻⁰⁴	1.43x10 ⁻²⁶	-100.00%	100.00%
810	6.70x10 ⁻⁰⁴	7.12x10 ⁻²⁷	-100.00%	100.00%
820	6.56x10 ⁻⁰⁴	3.54x10 ⁻²⁷	-100.00%	100.00%
830	6.42x10 ⁻⁰⁴	1.76x10 ⁻²⁷	-100.00%	100.00%
840	6.29x10 ⁻⁰⁴	8.72x10 ⁻²⁸	-100.00%	100.00%
850	6.16x10 ⁻⁰⁴	4.33x10 ⁻²⁸	-100.00%	100.00%
860	6.03x10 ⁻⁰⁴	2.15x10 ⁻²⁸	-100.00%	100.00%
870	5.90x10 ⁻⁰⁴	1.07x10 ⁻²⁸	-100.00%	100.00%
880	5.78x10 ⁻⁰⁴	5.30 x10 ⁻²⁹	-100.00%	100.00%
890	5.66x10 ⁻⁰⁴	2.63x10 ⁻²⁹	-100.00%	100.00%
900	5.54x10 ⁻⁰⁴	1.31x10 ⁻²⁹	-100.00%	100.00%
910	5.43x10 ⁻⁰⁴	6.49x10 ⁻³⁰	-100.00%	100.00%
920	5.31x10 ⁻⁰⁴	3.23x10 ⁻³⁰	-100.00%	100.00%
930	5.20x10 ⁻⁰⁴	1.60x10 ⁻³⁰	-100.00%	100.00%
940	5.09x10 ⁻⁰⁴	7.95x10 ⁻³¹	-100.00%	100.00%
950	4.99x10 ⁻⁰⁴	3.95x10 ⁻³¹	-100.00%	100.00%
960	4.88x10 ⁻⁰⁴	1.96x10 ⁻³¹	-100.00%	100.00%
970	4.78x10 ⁻⁰⁴	9.74x10 ⁻³²	-100.00%	100.00%
980	4.68x10 ⁻⁰⁴	4.84x10 ⁻³²	-100.00%	100.00%
990	4.58x10 ⁻⁰⁴	2.40x10 ⁻³²	-100.00%	100.00%
1000	4.49x10 ⁻⁰⁴	1.19x10 ⁻³²	-100.00%	100.00%
1010	4.39x10 ⁻⁰⁴	5.92x10 ⁻³³	-100.00%	100.00%
1020	4.30x10 ⁻⁰⁴	2.94x10 ⁻³³	-100.00%	100.00%
1030	4.21x10 ⁻⁰⁴	1.46x10 ⁻³³	-100.00%	100.00%
1040	4.12x10 ⁻⁰⁴	7.25x10 ⁻³⁴	-100.00%	100.00%
1050	4.04x10 ⁻⁰⁴	3.60x10 ⁻³⁴	-100.00%	100.00%
1060	3.95x10 ⁻⁰⁴	1.79x10 ⁻³⁴	-100.00%	100.00%
1070	3.87x10 ⁻⁰⁴	8.88x10 ⁻³⁵	-100.00%	100.00%
1080	3.79x10 ⁻⁰⁴	4.41 x10 ⁻³⁵	-100.00%	100.00%
1090	3.71x10 ⁻⁰⁴	2.19x10 ⁻³⁵	-100.00%	100.00%
1100	3.63x10 ⁻⁰⁴	1.09x10 ⁻³⁵	-100.00%	100.00%

Table A2: Percent Differences Between NCRP-156 Weak Retention Equation and Difference (i.m. - i.v.).